# Combination Multinitrogen with Good Oxygen Balance: Molecule and Synthesis Design of Polynitro-Substituted Tetrazolotriazine-Based Energetic Compounds

Piao He, Jian-Guo Zhang,* Kun Wang, Xin Yin, and Tong-Lai Zhang

State Key Laboratory of Explosion Science and Technology, Beijing Institute of Technology, Beijing 100081 P. R. China

Ⓢ Supporting Information

ABSTRACT: We investigated 5,8-dinitro-5,6,7,8-tetrahydrotetrazolo[1,5-*b*][1,2,4]triazine (short for DNTzTr (**1**)) using various ab initio quantum chemistry methods. We proposed an additional three novel polynitro-substituted tetrazolotriazine-based compounds with exceptional performance, including 5,8-dinitro-5,6-dioxotetrazolo[1,5-*b*][1,2,4]triazine, DNOTzTr (**2**), 4,5,9,10-tetranitro[1,2,4,5]tetrazolo[3,4-*b*][1,2,4,5]tetrazolo[3′,4′:5,6]triazino-[2,3-*e*]triazine, TNTzTr (**3**), and 4,5,6,10,11,12-hexanitro-bis-[1,2,4,5]tetrazolo[3′,4′:5,6]triazino[2,3-*b*:2′,3′-*e*]triazine, HNBTzTr (**4**). The optimized structure, electronic density, natural bond orbital (NBO) charges and HOMO−LUMO orbitals, electrostatic potential on surface of molecule, IR- and NMR-predicted spectra, as well as thermochemical parameters were calculated with the B3LYP/6-311+G(2d) level of theory. Critical parameters such as density, enthalpy of formation (EOF), and detonation performance have also been predicted. Characters with positive EOF (1386.00 and 1625.31 kJ/mol), high density (over 2.00 g/cm^3), outstanding detonation properties (D = 9.82 km/s, P = 45.45 GPa; D = 9.94 km/s, P = 47.30 GPa), the perfect oxygen balance set to zero, and acceptable impact sensitivity led novel compounds **3** and **4** to be very promising energetic materials. This work provides the theoretical molecule design and a reasonable synthesis path for further experimental synthesis and testing.
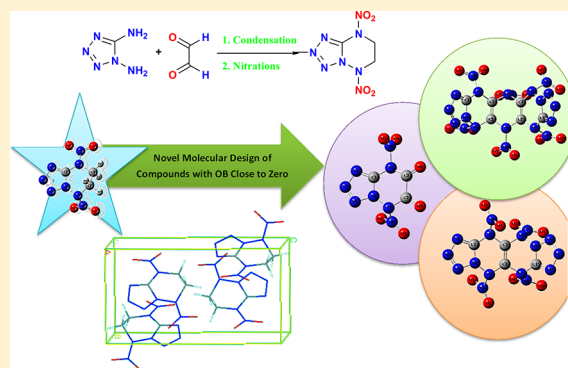
1. INTRODUCTION

The development of energetic materials[1,2] is an interesting and challenging area of chemistry from applied (such as explosives or propellants) and fundamental aspects, and it is important to discover new representatives with significant advantages over compounds currently used.[3] Desirable characteristics for high-energy density compounds (HEDCs) include good thermal stability, favorable insensitivity, remarkable explosive performance, and environmental acceptability.[4]

The performance of an energetic material depends mainly on its oxygen balance, density, and heat of formation, which are governed to some extent by the molecular structure.[5] On one hand, the lower oxygen balance leads to the poorer explosive performance and also does harm to the environment by releasing a large number of toxic gases and CO due to its incomplete combustion. On the other hand, the additional oxygen produces O$_2$ that will take away a great deal of energy during the explosion. Thus, one should keep the value of oxygen balance around zero in designing HEDCs.[3] Hexanitrohexaazaisowuritane (CL-20)[6] and octanitrocubane (ONC)[7,8] as excellent energetic CHNO substances possess strained rings, another characteristic with oxygen balance close to zero.

High-nitrogen compounds[9−11] represent a unique class of HEDCs, and the energy of most of these compounds mainly originates from the breaking and rearranging of the highly energetic bonds, including N−N (160 kJmol^{-1}), N=N (418 kJmol^{-1}), and N ≡ N (954 kJmol^{-1}) bonds, during the explosion.[3,12−14] A strong correlation between increasing explosive performance and, unfortunately, increasing sensitivity toward thermal and mechanical stimuli, can be observed.[15] Of these heterocycles, the tetrazole ring has been considered as the ideal balance point on the "stability versus performance continuum" for preparation of new energetic materials.[15]

Tetrazoles are frequently chosen for the design and synthesis of new energetic nitrogen-rich compounds.[16−23] 1,5-Diaminotetrazole (short for DAT) can act as a precursor for introducing the tetrazole ring into a wide range of energetic materials. In 1988, Willer reported the synthesis of the related 5,6,7,8-tetrahydrotetrazolo[1,5-*b*][1,2,4]triazines based on the reaction of DAT with glyoxals. Nitration proceeded smoothly in acetic anhydridelnitric acid to obtain the 5,8-dinitro compound (seen as DNTzTr (**1**) in Scheme 1) with six catenated nitrogen atoms, and the structure was confirmed by X-ray crystallography.[24] However, this interesting compound has negative oxygen balance, which may defuse the detonation performance.
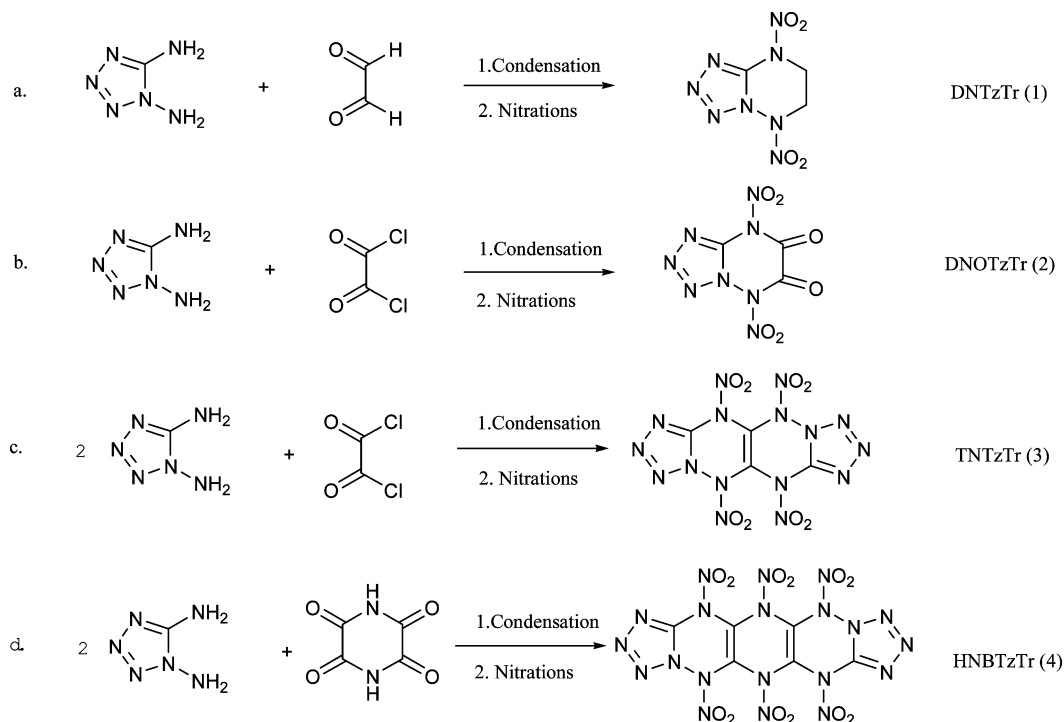
Scheme 1. Designed Novel Molecules of Polynitro-Substituted Tetrazolotriazine- Based Compounds

DNTzTr (1)   DNOTzTr (2)   TNTzTr (3)   HNBTzTr (4)
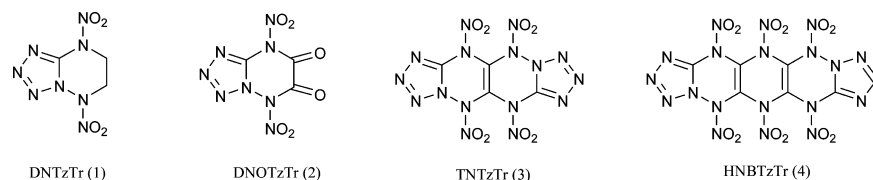
Scheme 2. Systematic Synthesis Paths of Title Compounds from 1,5-Diaminotetrazle (DAT)

To meet the continuing demand for improved energetic materials, there is a clear need to continue to design and develop new candidates with good performance and acceptable sensitivity. In this work, we attempted to design novel derivatives based on the combination of interesting energetic characteristics (oxygen balance close to zero) and unusual chemical structures (tetrazole ring). We first reported three novel compounds including 5,8-dinitro-5,6-dioxotetrazolo[1,5-b][1,2,4]triazine, DNOTzTr (2); 4,5,9,10-tetranitro[1,2,4,5]-tetrazolo[3,4-b][1,2,4,5]tetrazolo[3',4':5,6]triazino[2,3-e]-triazine, TNTzTr (3); 4,5,6,10,11,12-hexanitrobis[1,2,4,5]-tetrazolo[3',4':5,6]triazino[2,3-b:2',3'-e]triazine, HNBTzTr (4) (Scheme 1). Structures and properties of the promising compounds have been studied rigorously.

We also designed the reasonable synthesis path of title compounds based on the systematic synthesis method mainly including the condensation and nitration reactions (Scheme 2). The present theoretical study may simulate further experimental synthesis and testing of these novel high-nitrogen energetic compounds.

2. COMPUTATIONAL METHODS

All of the ab initio calculations involved in this work were carried out using the Gaussian 09[25] suite of programs. The structure optimizations of four title compounds have been performed using the hybrid DFT-B3LYP method with the 6-311+G(2d) basis set. Natural bond orbital (NBO)[26] charges, the highest occupied molecular orbitals (HOMO) and the lowest unoccupied molecular orbital (LUMO) orbitals,

electronic density, and electrostatic potential were calculated at the same level of theory. IR and NMR spectra and thermochemical parameters were obtained on the basis of the optimized gas-phase structure.

Enthalpy of formation is one of the most important parameters for energetic compounds. Atomequivalent schemes used to convert quantum mechanical energies of atoms to heats of formation of molecules can be given in terms of eq 1:[27]

$$\Delta H_f(g) = E(g) - \sum_i n_i x_i \tag{1}$$

Condensed-phase heats of formation can be determined using the gas-phase enthalpy of formation and enthalpy of phase transition (either sublimation or vaporization) according to Hess' law of constant heat summation[28]

$$\Delta H(\text{solid}) = \Delta H(\text{gas}) - \Delta H(\text{sublimation}) \tag{2}$$

$$\Delta H(\text{liquid}) = \Delta H(\text{gas}) - \Delta H(\text{vaporization}) \tag{3}$$

On the basis of the electrostatic potential of a molecule through quantum mechanical prediction, the enthalpy of sublimation either vaporization can be represented as[29,30]

$$\Delta H(\text{sublimation}) = a(\text{SA})^2 + b\sqrt{\sigma_{\text{tot}}^2 \upsilon} + c \tag{4}$$

$$\Delta H(\text{vaporization}) = a\sqrt{(\text{SA})} + b\sqrt{\sigma_{\text{tot}}^2 \upsilon} + c \tag{5}$$

where SA is the molecular surface area for this structure, σ_{tot}^2 is described as an indicator of the variability of the electrostatic potential on the molecular surface, and υ is interpreted as showing the degree of
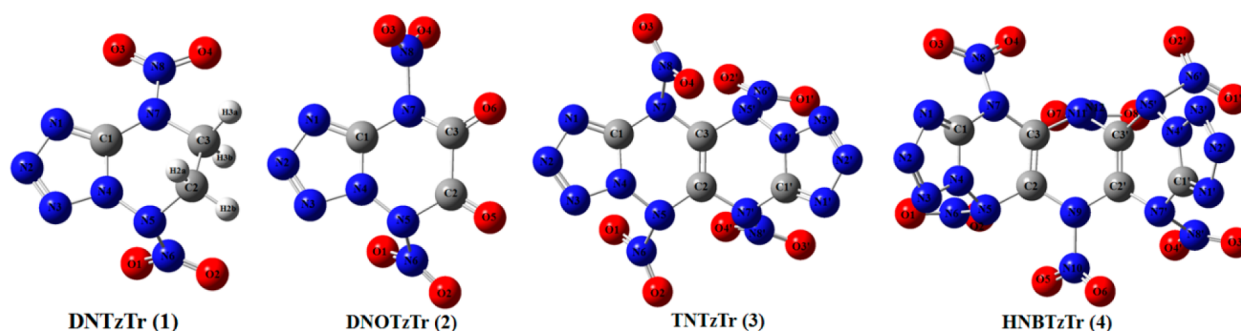
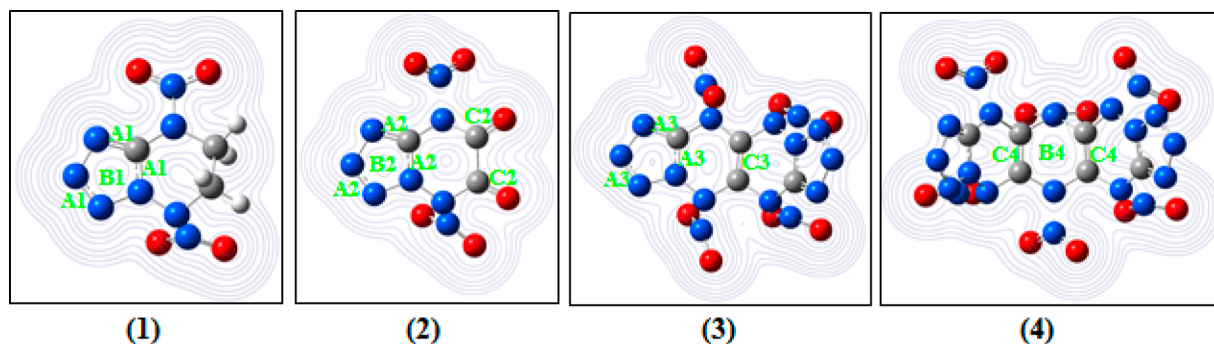**Figure 1.** Optimized structure of four title compounds.

Figure 2. Contour line map of electronic density on four title compounds.

balance between the positive and negative potentials on the molecular surface where a, b, and c are fitting parameters. We further followed the approach of Politzer et al. to predict solid and liquid enthalpy of formation combining these with eq 2 or eq 3.

The density, as another important parameter of energetic material, was obtained using an improved equation proposed by Politzer et al. considering intermolecular interactions within the crystal:[31]

$$\rho = \alpha\left(\frac{M}{V(0.001)}\right) + \beta(\nu\sigma^2_{tot}) + \gamma \qquad (6)$$

where $V(0.001)$ is the volume in cm^3/molecule and is encompassed by the 0.001 au contour of the electronic density, M is the molecular mass in g/molecule, $\nu\sigma^2_{tot}$ is derived from the molecular electrostatic potential calculation, and α, β, and γ were coefficients assigned through fitting eq 6 to the experimental densities of a series of 36 energetic compounds.[31]

The critical detonation parameters of energetic compounds including the detonation velocity and pressure were predicted by empirical Kamlet–Jacobs equations[32]

$$D = 1.01(N\bar{M}^{1/2}Q^{1/2})^{1/2}(1 + 1.30\rho) \qquad (7)$$

$$P = 1.558\rho^2 N\bar{M}^{1/2}Q^{1/2} \qquad (8)$$

where D is the detonation velocity (km/s), P is the detonation pressure (GPa), N is the moles of detonation gases per gram explosive, $\bar{M}$ is the average molecular weight of these gases, Q is the heat of detonation (cal/g), and ρ is the loaded density of explosives (g/cm^3) and is replaced by the theoretical density here.

Last but not least, the parameter for evaluating the energetic performance is the oxygen balance (OB), which is the index of the deficiency or excess of in a compound required to convert all carbon into carbon dioxide and all hydrogen into water. OB (%) for an explosive containing the general formula CaHbNcOd with molecular mass M_r can be calculated as[33]

$$OB = 1600 \times [d - 2a - b/2] \div M_r \qquad (9)$$

The bond dissociation energy (BDE) can be used to measure the relative order of thermal stability for energetic materials. The BDE here is defined as the difference between the zero-point-corrected energy of the parent molecules and that of fragments of the dissociation where an NO$_2$ group is removed, and the homolytic bond dissociation energy can be given as[34]

$$(BDE = E(A) + E(B) - E(AB) + \Delta ZPE) \qquad (10)$$

3. RESULTS AND DISCUSSION

3.1. Molecular Structure. The structure of DNTzTr (**1**) has been optimized using various ab initio methods including HF and B3LYP, and the basis sets include the split-valence types 6-31G(d), 6-311G(d), and 6-311+G(2d).[35,36] The geometrical parameters are not sensitive to the basis sets used in the optimization for B3LYP methods but depend on the ab initio methods. Using the HF method, the calculated NN and CN bonds lengths are shorter than the experimental data, while the distances of CC, ON, and CH bonds are a little longer. It is evident that the B3LYP results are close to the experiment compared with the HF, implying that the dynamical electron correlation plays a key role for the molecules of our concern. Thus, we performed all structure optimizations of the designed molecules by the B3LYP method with 6-311+G(2d) basis sets. The most stable conformations (shown in Figure 1) of the four title compounds are made of the tetrazole and triazine ring with polynitro, and all of them possess six catenated nitrogen atoms, which contributes to the explosive performance. The intact geometrical parameters are summarized in the Supporting Information.

Using the Multiwfn program[37] to calculate density, the contour line maps of electronic density on four title compounds are visualized in Figure 2. The heavy nuclei have high peaks caused by nuclear charge improving electron aggregation and then display integral exponential attenuation toward all around, and the electron densities around the oxygen and nitrogen atoms are higher than those around other atoms due to strong

electronegativity. The electrons prefer to assemble in the bonding area (such as A1, A2, and A3) because of electron pair sharing between atoms with covalence interaction. For molecules of both **1** and **2**, the delocalization mainly occurs in the tetrazole ring (such as B1 and B2), which may improve the stability of the ring skeleton, and large electrons also assemble between carbon and oxygen atoms, allowing for a forming C=O bond in the molecule of **2**. For **3** and **4**, the areas marked as C3 and C4 suggest their nature of covalent bonding derived from the π orbitals over the C=C bonds. The delocalization also occurs in the central ring of **4** (such as B4) from the electron distribution.

3.2. Natural Bond Orbital. Natural bond orbital analysis is an essential tool for studying interactions among bonds.[38] NBO charges are summarized in the Supporting Information. The majority of negative charges are localized on the oxygen atom and partial nitrogen atom, whereas the positive charges are located on the carbon atom due to the difference of electronegativity. The N6 and N8 atoms in nitro group accommodate positive charges as result of electron departure toward the oxygen atom. Moreover, the negative charges both on nitrogen and oxygen atoms of **3** and **4** are decreased compared with **1** and **2**, which is attributed to the mutual effect among electrons of large nitro groups in molecules.

The energy gap between HOMO and LUMO relates the kinetic stability, chemical reactivity, and optical polarizability of a molecule.[39] HOMO and LUMO orbitals including the energy gap are depicted in Figure 3, and the positive phase is red and the negative one is green. As can be seen from Figure 3, the HOMO is localized approximately on the tetrazole ring and the LUMO is localized on the substituted groups around the rings. The values of energy separation between the HOMO and LUMO are 5.1307, 4.5829, 3.3410, and 1.2019 eV for title compounds **1**, **2**, **3**, and **4**, respectively. Therefore, the predicted sequence of chemical activity is **4 > 3 > 2 > 1**, which is the reverse order of stability for title compounds as well.

3.3. ESP on Molecular Surface. Electrostatic potential (ESP)[40] on the molecular surface gives more meaningful insight into charge distributions and is useful for understanding intermolecular interaction.[41] The ESP-mapped vdW surfaces of four title molecules are shown in Figure 4. Significant surface local minima and maxima of ESP are represented as cyan and orange spheres and labeled by dark blue and brown-red texts with the unit in kcal/mol. Only the global minima and maxima on the surface are labeled by italic font. The surface areas in each ESP range are plotted in Figure 5.

It can be seen from Figure 4, in the unit regions of molecules **1** and **2**, that the surface minima of ESP are present between nitrogen and oxygen atoms, especially on the N1, N2, and N3 atoms of the tetrazole ring, which are the primary electrophilic sites. The surface maximum prefer to carbon and hydrogen atoms, which illustrates that the nucleophile attack might be easier. The global maxima of ESP are +49.86 and +65.53 kcal/mol for **1** and **2**, corresponding to the carbon and hydrogen in the triazine part, and the global minima are −38.02 and −25.48 kcal/mol, corresponding to the nitrogen atoms. For the molecules **3** and **4**, the surface maxima of ESP are distributed near carbon atoms (C2, C3) and the minima are distributed nitrogen atoms (N1, N2, N3), respectively. The global maxima and minima of ESP are +56.73 and −24.87 kcal/mol for **3** and +58.80 and −25.00 kcal/mol for **4**, corresponding to the carbon of central ring and the nitrogen of tetrazole.

The results from Figure 5 show that molecule **1** unit has a surface with ESP value (i.e., within −30 to +40 kcal/mol) and most surfaces of molecule **2** unit have ESP value (i.e., within −20 to +30 kcal/mol). The area of positive ESP on the **1** unit is larger than that of the **2** unit due to the existence of hydrogen atoms of **1**. Both **3** and **4** units have most of their surface with ESP value (i.e., within −15 to +30 kcal/mol) as a shape of "high middle and low sides". The biggest surface area has an ESP of +5 kca/mol, which corresponds to the central ring, and the small surface has an ESP of −20 kcal/mol, which corresponds to the tetrazole.

3.4. Vibration Analysis and NMR. IR spectrum is an effective method to identify the substances. The characteristic peaks from simulated infrared results are shown in Figure 6, and comprehensive data are listed in the Supporting Information. The strong IR peaks at 1685 and 1653 cm^{-1} of compound **1** correspond to the asymmetrical stretching modes of the nitro groups, and the peaks at 1292 cm^{-1} refer to symmetrical stretching. As for compound **2**, two stronger peaks at 1839 and 1819 cm^{-1} are assigned to symmetrical stretching of C=O bonds in the triazine ring, while the weaker ones at 1591 and 1469 cm^{-1} are stretching vibrations on CN and NN of the tetrazole skeleton. The strongest peaks at 1354 cm^{-1} of compound **3** are mainly dominated by the symmetrical stretching on nitro groups. The peaks at 1578 and 1397 cm^{-1} correspond to the symmetrical stretching and torsion modes on the C=C bond. The characteristic peaks at 1847−769 cm^{-1} for compound **4** refer to the asymmetrical and symmetrical stretching and the torsion vibration modes of the nitro groups, and the weakest one at 1581 cm^{-1} refers to the symmetrical stretching on the C=C bonds of the central ring.
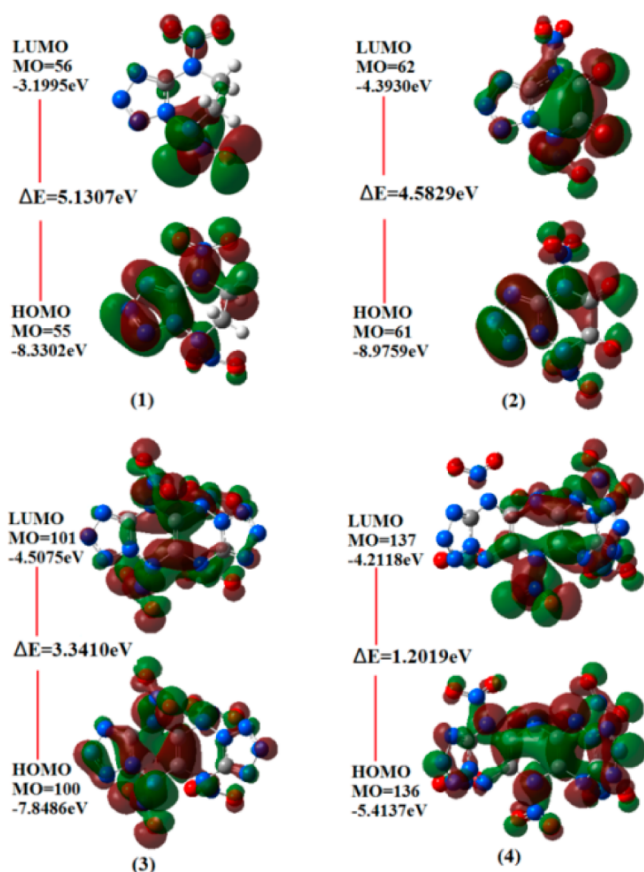
Figure 3. HOMO and LUMO orbitals of four title compounds.

LUMO MO=56 −3.1995eV

ΔE=5.1307eV

HOMO MO=55 −8.3302eV

(1)

LUMO MO=62 −4.3930eV

ΔE=4.5829eV

HOMO MO=61 −8.9759eV

(2)

LUMO MO=101 −4.5075eV

ΔE=3.3410eV

HOMO MO=100 −7.8486eV

(3)

LUMO MO=137 −4.2118eV

ΔE=1.2019eV
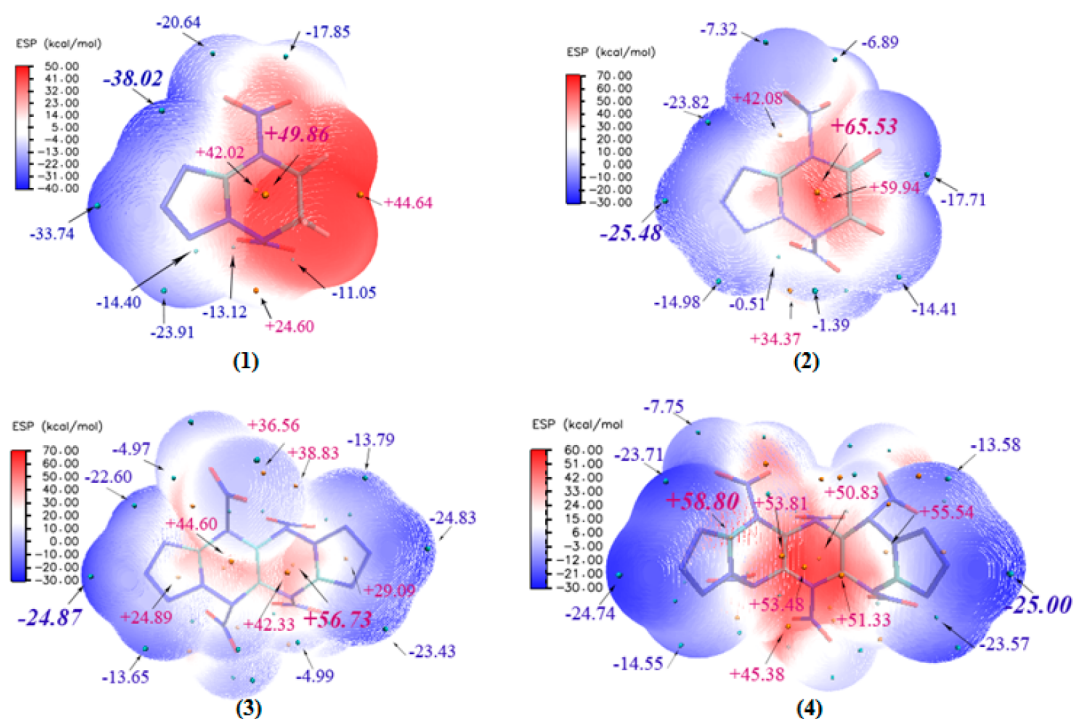
HOMO MO=136 −5.4137eV

(4)

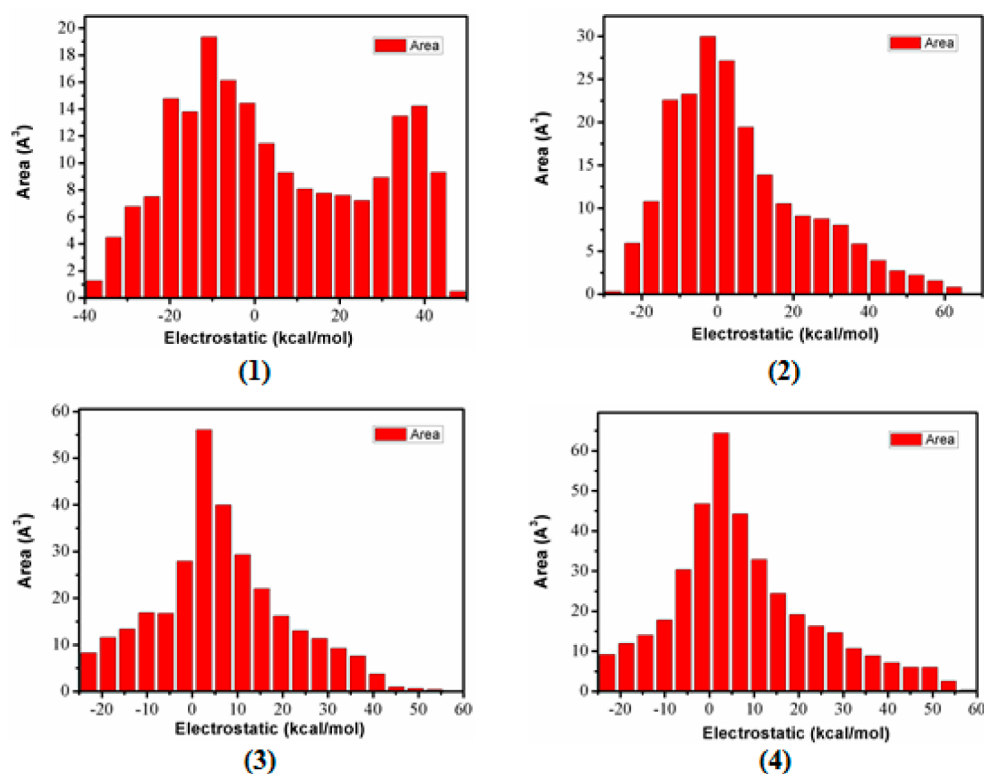**Figure 4.** ESP-mapped molecular vdW surface of four title compounds.

Figure 5. Area percent in each ESP range of four title compounds.

It is worth being noticed that the variances of IR spectrum vibrations on nitro groups in different positions can be observed in the four title compounds.

Thermochemical parameters, including internal energy (U), enthalpy (H), free energy (G), constant volume molar heat capacity (C_v), and molar entropy (S), of title compounds were evaluated and tabulated in Table 1.

The calculations of molecular properties play an important role, especially if they complement experiments with the information on molecular and electronic structure as it is the case in NMR spectroscopy.[42] The theoretical chemical shifts of C and H in ppm in ^{1}H and ^{13}C NMR relative to Me$_4$Si and chemical shifts of N in ^{15}N NMR to MeNO$_2$ have been calculated as shown in Table 2. The IR, thermochemical
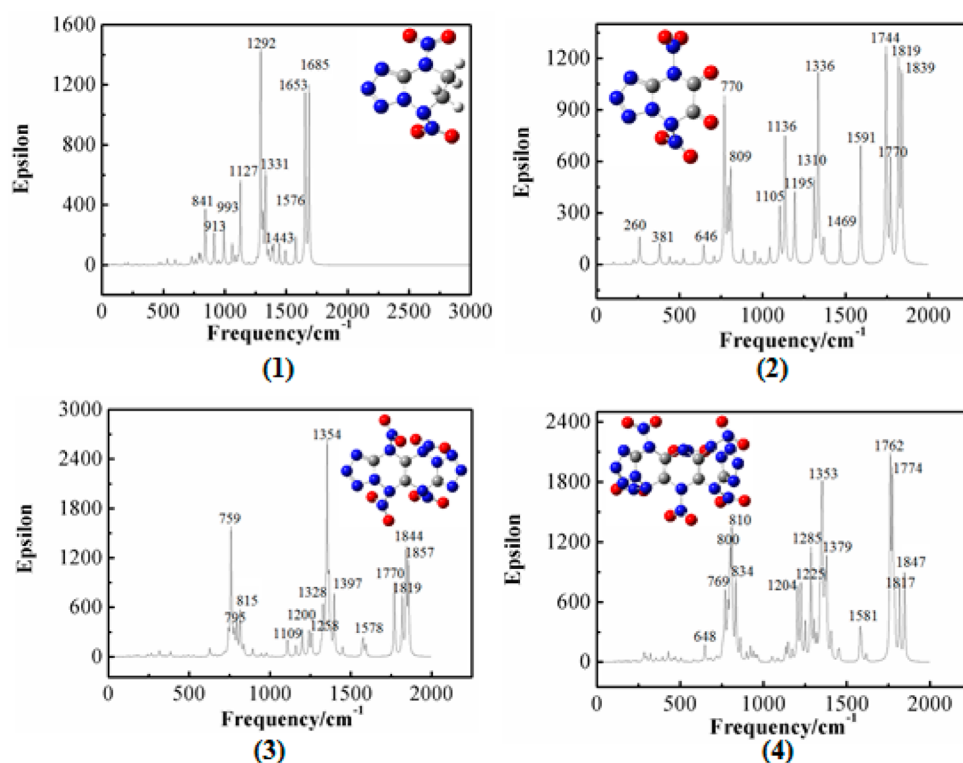
Figure 6. Calculated IR spectrum of four title compounds.

Table 1. Thermochemical Parameters of Four Title Compounds (at 298.15 K and 1.00 atm)

species	U (kcal/mol)	H (kcal/mol)	G (kcal/mol)	S (kcal/(mol·K))	C_v (kcal/(mol·K))
1	82.29	82.88	50.12	109.89	42.59
2	58.00	58.59	21.89	123.09	47.85
3	98.06	98.66	48.78	167.27	79.33
4	134.23	134.82	74.38	202.71	109.05

Table 2. Calculated ^{1}H, ^{13}C, and ^{15}N NMR Data for Four Title Compounds

^{1}H NMR						
H2a	3.40	H2b	5.25	H3a	4.41	H3b	3.67

^{13}C NMR			
	compd **1**	compd **2**	compd **3**	compd **4**
C1	156.00	154.71	161.45	159.50
C2	41.92	156.22	138.04	133.99
C3	47.32	153.40	144.22	122.62
C1′			162.64	160.79
C2′				136.61
C3′				120.79

^{15}N NMR								
compd **1**		compd **2**		compd **3**				compd **4**			
N1	−163.29	N1	−58.07	N1	−145.72	N1′	−122.17	N1	−142.99	N1′	−124.84
N2	−7.98	N2	−235.13	N2	5.05	N2′	3.86	N2	5.99	N2′	7.68
N3	−70.43	N3	−169.87	N3	−61.59	N3′	−46.87	N3	−60.45	N3′	−54.12
N4	−271.37	N4	40.13	N4	−249.57	N4′	−248.51	N4	−244.90	N4′	−246.13
N5	−267.86	N5	−26.51	N5	−187.99	N5′	−245.39	N5	−253.95	N5′	−211.37
N6	−45.97	N6	−153.78	N6	−43.92	N6′	−56.58	N6	−53.23	N6′	−55.70
N7	−312.67	N7	18.21	N7	−229.26	N7′	−293.21	N7	−291.65	N7′	−300.20
N8	−68.72	N8	−130.33	N8	−73.87	N8′	−62.73	N8	−84.10	N8′	−64.96
								N9	−265.57	N11	−287.73
								N10	−89.76	N12	−43.37

Table 3. Enthalpies of Formation, Enthalpy of Vaporization, and Enthalpy of Sublimation (kJ/mol) and Density

species[a]	$\Delta_f H$ (gas)	$\Delta_f H$ (liquid)	$\Delta_f H$ (solid)	ΔH (vap)	ΔH (sub)	ρ (g/cm^3)
TNT[44]	24.035		−63.12		104.50	1.64
RDX[44]	191.44		79.00		112.02	1.80
HMX[44]			75.24			1.90
FOX-7[45]			−133.70			1.89
1	619.72	538.31	497.64	81.41	122.08	1.815
2	497.39	423.31	387.44	74.08	109.95	1.97
3	1586.34	1488.12	1386.00	98.22	200.34	2.00
4	1928.71	1812.48	1625.31	116.23	303.40	2.05

[a]TNT, trinitrotoluene; RDX, cyclotrimethylene trinitramine; HMX, cyclotetramethylene tetranitramine; FOX-7, 1,1-diamino-2,2-dinitroethene.

Table 4. Detonation Parameters for Common HEDMs and Title Compounds

species[a]	$\Delta_f H_{298K}$(s) (kJ/mol)	Q (cal/g)	ρ (g/cm^3)	D (km/s)	P (GPa)	OB (%)
TNT[46]	−63.12	1295	1.64	6.95	19.00	−74.00
RDX[46]	79.00	1501	1.80	8.75	34.70	−21.62
HMX[46]	102.41	1498	1.90	9.10	39.30	−21.62
PETN[46]	−128.70	1514	1.77	8.30	33.50	−10.12
TATB[46]	−17.85	1149	1.89	7.86	31.50	−55.81
FOX-7[46]	−133.70	1200	1.89	8.87	34.00	−21.62
CL-20[46]	377.04	1567	2.04	9.38	44.10	−10.96
ONC[45]	392.92		1.98	9.50	46.00	0
1	497.64	1520	1.82	8.73	33.97	−29.63
2	387.44	1535	1.97	9.26	40.07	0
3	1386.00	1768	2.00	9.82	45.45	0
4	1625.31	1751	2.05	9.94	47.30	0

[a]TNT, trinitrotoluene; RDX, cyclotrimethylene trinitramine; HMX, cyclotetramethylene tetranitramine; PETN, tetranitrate pentaerythritol; TATB, 2,4,6-trinitro-1,3,5-benzenetriamine; FOX-7, 1,1-diamino-2,2-dinitroethene; CL-20, hexanitrohexaazaisowuritane; ONC.

parameters, and NMR were predicted for easier assignment and positive identification of the four target compounds.

3.5. Enthalpy of Formation and Density. Enthalpy of formation (EOF) is an important parameter, and it indicates the energy content of a material. High density is desirable in terms of the energetic material that can be packed into volume-limited warheads or propulsion configurations.[43] Calculated EOF and density for title compounds and common explosives are summarized in Table 3.

It is evidently important to use solid-state enthalpies of formation to predict the detonation performance of energetic compounds. Some compounds in Table 3 actually possess negative enthalpies of formation due to the large enthalpy of phase transition, such as TNT and RDX. However, a strongly positive enthalpy of formation is considered as very desirable property to increase detonation heat, which is the main reason for the interest in high nitrogen compounds. Quite noteworthy in this respect are compound 3 and 4 with the most positive enthalpy of formation (1386.00 and 1625.31 kJ/mol) than that of other common explosives. In addition, the predicted densities of 2−4 have been found to be in the range of 1.97−2.05 g/cm^3, which are much higher than those of TNT, RDX, HMX, and FOX-7. It is gratifying that 3 and 4 show the highest density of about 2.00 and 2.05 g/cm^3 among all the compounds studied, and this may be as result of incorporating nitro groups into the designing molecule species. It can be expected that high density and positive enthalpy of formation are very beneficial to improving the detonation velocity and pressure.

3.6. Detonation Properties. The detonation parameters for a few HEDMs have been calculated including the detonation heat (Q), detonation velocity (D) and pressure

(P), and oxygen balance (OB). Table 4 listed the systemic data of title compounds and eight famous explosives for comparison.

All of the title compounds possess a very high EOF derived from the large number of inherently energetic C−N and N−N bonds in molecules, and the density of 4 is up to 2.05 g/cm^3, which is even similar to excellent CL-20 (2.04 g/cm^3). The most characteristic in three designed compounds is that the OB is close to zero, which may make for the heat releases in detonation by sufficient oxidation. As a result, the heats of detonation of 3 and 4 are about 1768 and 1751 cal/g, which become the highest ones among all the compounds. Detonation velocity and detonation pressure as two important performance parameters for an energetic compound are compared in Table 4. It is greatly surprising that three new compounds 2−4 own higher D and P than HMX as commonly used energetic ingredients. It should be noticed that compounds 3 and 4 have very remarkable detonation performance with D = 9.82 km/s, P = 45.45 GPa, D = 9.94 km/s, and P = 47.30 GPa, which are much greater than excellent explosive CL-20. Overall, all designed compounds with perfect oxygen balance possess extremely fascinating detonation properties, and they might be the most promising energetic materials among the CHNO-containing organic compounds.

3.7. Stability and Sensitivity. Bond dissociation energy (BDE) provides useful information for understanding the stability of the title compounds. There is evidence that the weakest bond in polynitro compounds is the R−NO$_2$ bond and that rupture of this bond is the first step in decomposition,[47] so the BDEs and Wiberg bond order of significant N−NO$_2$ bond scission for title compounds were calculated in detail. It is found that the N−NO$_2$ bonds have slightly different BDE

values because of the asymmetric structure and the position of the substituent in different molecules, and compounds **1** and **2** basically have higher BDE than derivatives **3** and **4**, which indicates that the increasing nitro substituent could decrease the thermal stability. Most of the dissociation energies and bond orders show the corresponding trend that the greater the bond order, the larger the corresponding BDE. The weakest bond N−NO$_2$ for four title compounds **1**, **2**, **3**, and **4** is N5−N6 (27.64 kcal/mol, 0.84), N7−N8 (18.28 kcal/mol, 0.75), N5−N6 (2.06 kcal/mol, 0.49), and N5′−N6′ (8.44 kcal/mol, 0.58) from the BDE and bond order values. This predicts that the trigger linkage of decomposition appears to these bonds, whereas other bonds are relatively strong and resistant to rupture.

The sensitivities of energetic materials play a key role in determining their potential application and handling safety.[48] The impact sensitivity is by far the most common method of assessing sensitivities of an explosive and measured by the $h_{50\%}$, namely the height from where 50% probability of the "drops" result in reaction of the sample. Several strong correlations have been found that relate impact sensitivities with various molecular properties, particularly within chemical families.[45,49−54] Employing quantum chemistry and molecular dynamics methods, Rice and Hare[52] used the statistical parameters related to features of surface electrostatic potentials and the property-structure relation method "generalized interaction property function" (GIPF) or the heats of detonation to estimate impact sensitivity of CaHbNcOd explosives. Four introduced models based on the GIPF parameters have been performed in this work to predict the $h_{50\%}$ values of title compounds, and the results are listed in Table 5.

Table 5. Predicted and Experimental $h_{50\%}$ Values (cm) for Molecules Studied

compd[a]	method 1[b]	method 2[c]	method 3[d]	method 4[e]	expt[f]
TNT	73	80	133	143	98
RDX	49	31	39	22	28
HMX	21	31	41	22	32
PETN	28	30	41	16	13
TATB	498	307	502	478	490
FOX-7	320	40	168	133	126
CL-20	16	29	29	3	14
1	36	73	28	5	
2	42	30	28	2	
3	80	55	28	0.9	
4	75	33	28	0.7	

[a]All $h_{50\%}$ values of common explosives are reported in ref 52 except those calculated for the title compounds. [b]Method 1 is based on the GIPF parameters $\overline{V_S^-}$ and $\overline{V_S^+}$. [c]Method 2 is based on the GIPF balance parameter ν. [d]Method 3 is based on the heat of detonation Q. [e]Method 4 is based on the hybrid model using Q and ν. [f]The partial experimental values derive from ref 52.

Although these models might be limited in their predictive capability, the predictions could distinguish between a CHNO explosive and nonexplosive. Among the suggested four methods, methods 1−3 show relatively consistent results, while method 4 greatly overestimates impact sensitivities originated from the hybrid heat of detonation and balance parameter, and the impact sensitivity increases with the relative numbers of nitro groups in molecules. We estimated $h_{50\%}$ values

of four title compounds to be about 28 cm, and these designed energetic compounds seem to have the similar impact sensitivity as RDX (28 cm), HMX (32 cm), and CL-20 (14 cm). However, because of the complexity of the impact sensitivity, the accuracy of the predictions from the models could not be assured entirely.

4. CONCLUSION

In this work, we studied on the 5,8-dinitro-5,6,7,8-tetrahydrotetrazolo[1,5-*b*][1,2,4]triazine (short for DNTzTr, **1**) by using various ab initio quantum chemistry methods, and three novel polynitro-substituted tetrazolotriazine-based compounds including DNOTzTr (**2**), TNTzTr (**3**), HNBTzTr (**4**) have been proposed first and investigated at the B3LYP/6-311+G(2d) level of theory.

The optimized molecular structures possess six catenated nitrogen atoms and are dominated by the tetrazole and triazine ring with polynitro as energetic groups. Again the significant surface local minima and maxima of ESP provide a visual representation of the chemically active sites. The calculated thermochemical parameters, IR and NMR spectrum data have been performed for easier assignment and positive identification of the target compounds. Very noteworthy in this respect are designed compound (**3**) and (**4**) with the most positive EOF (1386.00 and 1625.31 kJ/mol) and high densities over 2.00 g/cm^3. They also possess very remarkable detonation parameters with D = 9.82 km/s, P = 45.45 GPa and D = 9.94 km/s, P = 47.30 GPa, which are comparable with excellent explosive ONC, and that novel designed compound **3** and **4** might be very promising high-energy density compounds based on so much outstanding characteristics. Since the impact sensitivities of these compounds are similar to RDX, HMX, and CL-20, they could be considered to be primary explosives and should only be handled with appropriate precautions.

Our observations indicate that combination of the tetrazole derivatives and oxygen balance to zero is a very effective way to obtain potential energetic compounds with outstanding detonation performance. We expect the relative theoretical work including this design concept of molecule and synthesis could promote the synthesis of new high-nitrogen materials in the foreseeable future.

■ ASSOCIATED CONTENT

Ⓢ Supporting Information

Optimized parameters, NBO charges, and IR spectrum analysis of the four title compounds. The Supporting Information is available free of charge on the ACS Publications website at DOI: 10.1021/acs.joc.5b00545.

■ AUTHOR INFORMATION

Corresponding Author

*Tel/Fax: +86 10 68918091. E-mail: zjgbit@bit.edu.cn.

Notes

The authors declare no competing financial interest.

■ ACKNOWLEDGMENTS

■ REFERENCES

(1) Zhang, S.; Liu, X.; Yang, Q.; Su, Z.; Gao, W.; Wei, Q.; Xie, G.; Chen, S.; Gao, S. *Chem.—Eur. J.* **2014**, *20*, 7906−7910.

(2) Zhang, Q.; Shreeve, J. M. *Angew. Chem., Int. Ed.* **2014**, *53*, 2540−2542.

(3) Gao, H.; Shreeve, J. M. *Chem. Rev.* **2011**, *111*, 7377−7436.

(4) Thottempudi, V.; Gao, H.; Shreeve, J. M. *J. Am. Chem. Soc.* **2011**, *133*, 6464−6471.

(5) Wu, Q.; Zhu, W.; Xiao, H. *J. Chem. Eng. Data* **2013**, *58*, 2748−2762.

(6) Geetha, M.; Nair, U. R.; Sarwade, D. B.; Gore, G. M.; Asthana, S. N.; Singh, H. *J. Therm. Anal. Calorim.* **2003**, *73*, 913−922.

(7) Schmidt, S.; Bauer, W.; Heinemann, F. W.; Lanig, H.; Grohmann, A. *Angew. Chem., Int. Ed.* **2000**, *39*, 913−916.

(8) Lukin, K. A.; Li, J.; Eaton, P. E.; Kanomata, N.; Hain, J.; Punzalan, E.; Gilardi, R. *J. Am. Chem. Soc.* **1997**, *119*, 9591−9602.

(9) Hirshberg, B.; Gerber, R. B.; Krylov, A. I. *Nat. Chem.* **2014**, *6*, 52−56.

(10) Qin, J.-S.; Du, D.-Y.; Li, W.-L.; Zhang, J.-P.; Li, S.-L.; Su, Z.-M.; Wang, X.-L.; Xu, Q.; Shao, K.-Z.; Lan, Y.-Q. *Chem. Sci.* **2012**, *3*, 2114−2118.

(11) Heppekausen, J.; Klapötke, T. M.; Sproll, S. M. *J. Org. Chem.* **2009**, *74*, 2460−2466.

(12) Klapötke, T. M.; Stierstorfer, J. *J. Am. Chem. Soc.* **2009**, *131*, 1122−1134.

(13) Joo, Y.-H.; Twamley, B.; Garg, S.; Shreeve, J. M. *Angew. Chem., Int. Ed.* **2008**, *47*, 6236−6239.

(14) Klapötke, T. M., In *Chemistry of High-Energy Materials*, 2nd ed.: Walter de Gruyter: Berlin, 2011; Chapter 9.2, pp 153−160.

(15) Fischer, D.; Klapötke, T. M.; Piercey, D. G.; Stierstorfer, J. *Chem.—Eur. J.* **2013**, *19*, 4602−4613.

(16) Singh, R. P.; Verma, R. D.; Meshri, D. T.; Shreeve, J. n. M. *Angew. Chem., Int. Ed.* **2006**, *45*, 3584−3601.

(17) Liu, Z.; Wu, Q.; Zhu, W.; Xiao, H. *J. Phys. Org. Chem.* **2013**, *26*, 939−947.

(18) Lin, Q.-H.; Li, Y.-C.; Qi, C.; Liu, W.; Wang, Y.; Pang, S.-P. *J. Mater. Chem. A* **2013**, *1*, 6776.

(19) Klapötke, T. M.; Martin, F. A.; Stierstorfer, J. *Chem.—Eur. J.* **2012**, *18*, 1487−1501.

(20) Klapötke, T. M.; Krumm, B.; Martin, F. A.; Stierstorfer, J. *Chem.—Asian J.* **2012**, *7*, 214−224.

(21) Hiskey, M. A.; Goldman, N.; Stine, J. R. *J. Energy Mater.* **1998**, *16*, 119−127.

(22) Fischer, N.; Klapötke, T. M.; Reymann, M.; Stierstorfer, J. *Eur. J. Inorg. Chem.* **2013**, *2013*, 2167−2180.

(23) Abe, T.; Tao, G.-H.; Joo, Y.-H.; Huang, Y.; Twamley, B.; Shreeve, J. n. M. *Angew. Chem., Int. Ed.* **2008**, *47*, 7087−7090.

(24) Willer, R. L.; Henry, R. A. *J. Org. Chem.* **1988**, *53*, 5371−5374.

(25) Frisch, M. J.; Trucks, G. W.; Schlegel, H. B.; Scuseria, G. E.; Robb, M. A.; Cheeseman, J. R.; Montgomery, J. A., Jr.; Vreven, T.; Kudin, K. N.; Burant, J. C.; Millam, J. M.; Iyengar, S. S.; Tomasi, J.; Barone, V.; Mennucci, B.; Cossi, M.; Scalmani, G.; Rega, N.; Petersson, G. A.; Nakatsuji, H.; Hada, M.; Ehara, M.; Toyota, K.; Fukuda, R.; Hasegawa, J.; Ishida, M.; Nakajima, T.; Honda, Y.; Kitao, O.; Nakai, H.; Klene, M.; Li, X.; Knox, J. E.; Hratchian, H. P.; Cross, J. B.; Bakken, V.; Adamo, C.; Jaramillo, J.; Gomperts, R.; Stratmann, R. E.; Yazyev, O.; Austin, A. J.; Cammi, R.; Pomelli, C.; Ochterski, J. W.; Ayala, P. Y.; Morokuma, K.; Voth, G. A.; Salvador, P.; Dannenberg, J. J.; Zakrzewski, V. G.; Dapprich, S.; Daniels, A. D.; Strain, M. C.; Farkas, O.; Malick, D. K.; Rabuck, A. D.; Raghavachari, K.; Foresman, J. B.; Ortiz, J. V.; Cui, Q.; Baboul, A. G.; Clifford, S.; Cioslowski, J.; Stefanov, B. B.; Liu, G.; Iiskorz, P.; Komaromi, I.; Martin, R. L.; Fox, D. J.; Keith, T.; Al-Laham, M. A.; Peng, C. Y.; Nanayakkara, A.; Challacombe, M.; Gill, P. M. W.; Johnson, B.; Chen, W.; Wong, M. W.; Gonzalez, C.; Pople, J. A. *Gaussian 9 (Revision A.01)*; Gaussian, Inc., Wallingford, CT, 2009.

(26) Weinhold, F.; Landis, C. R. *Chem. Educ.: Res. Pract. Eur.* **2001**, *2*, 91−104.

(27) Byrd, E. F.; Rice, B. M. *J. Phys. Chem. A* **2006**, *110*, 1005−1013.

(28) Atkins, P. W. *Physical Chemistry*; Oxford University Press: Oxford, 1982.

(29) Politzer, P.; Murray, J. S.; Brinck, T.; Lane, P. *Immunoanalysis of Agrochemicals.*; ACS Sympsium Series 586; American Chemical Society: Washington, DC, 1994.

(30) Murray, J. S.; Politzer, P. In *Quantitative Treatment of Solute/Solvent Interactions, Theoretical and Computational Chemistry*; Elsevier: Amsterdam, 1994.

(31) Politzer, P.; Martinez, J.; Murray, J. S.; Concha, M. C.; Toro-Labbé, A. *Mol. Phys.* **2009**, *107*, 2095−2101.

(32) Kamlet, M. J.; Jacobs, S. J. *J. Chem. Phys.* **1968**, *48*, 23−35.

(33) Thottempudi, V.; Shreeve, J. n. M. *J. Am. Chem. Soc.* **2011**, *133*, 19982−19992.

(34) Blanksby, S. J.; Ellison, G. B. *Acc. Chem. Res.* **2003**, *36*, 255−263.

(35) Ditchfield, R.; Hehre, W. J.; Pople, J. A. *J. Chem. Phys.* **1971**, *54*, 724−728.

(36) Frisch, M. J.; Pople, J. A.; Binkley, J. S. *J. Chem. Phys.* **1984**, *80*, 3265−3269.

(37) Lu, T.; Chen, F. *J. Comput. Chem.* **2012**, *33*, 580−592 (http://Multiwfn.codeplex.com).

(38) James, C.; Raj, A. A.; Reghunathan, R.; Jayakumar, V. S.; Joe, I. H. *J. Raman Spectrosc.* **2006**, *37*, 1381−1392.

(39) Kosar, B.; Albayrak, C. *Spectrochim. Acta, Part A* **2011**, *78*, 160−167.

(40) Politzer, P.; Murray, J. S. *Theor. Chem. Acc.* **2002**, *108*, 134−142.

(41) Murray, J. S.; Politzer, P. *Comp. Mol. Sci.* **2011**, *1*, 153−163.

(42) Auer, A. A. *Chem. Phys. Lett.* **2009**, *467*, 230−232.

(43) Ghule, V. D. *J. Phys. Chem. C* **2013**, *117*, 16840−16849.

(44) Rice, B. M.; Pai, S. V.; Hare, J. *Combust. Flame* **1999**, *118*, 445−458.

(45) Song, X.; Li, J.; Hou, H.; Wang, B. *J. Comput. Chem.* **2009**, *30*, 1816−1820.

(46) Politzer, P.; Murray, J. S. *Cent. Eur. J. Energy Mater.* **2011**, *8*, 209−220.

(47) Rice, B. M.; Sahu, S.; Owens, F. J. *THEOCHEM* **2002**, *583*, 69−72.

(48) Sikder, A. K.; Sikder, N. *J. Hazard. Mater.* **2004**, *112*, 1−15.

(49) Zhang, J.; Shreeve, J. n. M. *J. Am. Chem. Soc.* **2014**, *136*, 4437−4445.

(50) Hirshberg, B.; Denekamp, C. *Phys. Chem. Chem. Phys.* **2013**, *15*, 17681−17688.

(51) Keshavarz, M. H. *J. Hazard. Mater.* **2007**, *148*, 648−652.

(52) Rice, B. M.; Hare, J. J. *Phys. Chem. A* **2002**, *106*, 1770−1783.

(53) Klapoetke, T. M.; Krumm, B.; Ilg, R.; Troegel, D.; Tacke, R. *J. Am. Chem. Soc.* **2007**, *129*, 6908−6915.

(54) Thottempudi, V.; Shreeve, J. n. M. *J. Am. Chem. Soc.* **2011**, *133*, 19982−19992.